Plasma Chemistry and Plasma Processing (2023) 43:709–736
https://doi.org/10.1007/s11090-023-10319-w

ORIGINAL PAPER

Cell Attachment and Laminin Immobilization on Hydrogels Coated by Plasma Deposited Nitrogen, Oxygen or Sulfur Based Organic Thin Films

Bishakh Rout[1] · **Pierre-Luc Girard-Lauriault**[1]

Received: 1 September 2022 / Accepted: 3 February 2023 / Published online: 18 March 2023

Abstract
Hydrogels are surfaces suitable for use as biomedical devices. Contact lenses are commonly used biomedical devices made from hydrogels. To enhance the application of contact lenses as cell delivery options, surface modification using low-pressure plasma enhanced chemical vapor deposition. The study investigated cell attachment on a few types of plasma deposited organic films: two types each of pure ethylene plasma polymer films, O-rich, N-rich and S-rich films on top of the hydrogels. The films led to changes in wettability, protein adsorption and the mechanical properties of the hydrogel surfaces, which are factors affecting cell proliferation. These films were also investigated for stability towards steam sterilisation Finally, these films stable towards water exposure and steam sterilisation were used to immobilize laminin in order to improve cell proliferation. The study investigated the possibility of using surface modified contact lenses could to deliver cell therapies to the eye environment.

Keywords Hydrogels · Plasma polymer films · Cell attachment · Protein adsorption · Surface modification

Abbreviations

CL	Contact lens
PPF	Plasma polymer film
R-LEC	Rabbit lens epithelial cells
PPE	Plasma polymerised ethylene
PPB	Plasma polymerised butadiene

✉ Pierre-Luc Girard-Lauriault
pierre-luc.girard-lauriault@mcgill.ca

[1] Plasma Chemical Processing Laboratory, Department of Chemical Engineering, McGill University, Montreal H3A 0C5, Canada

Introduction

Hydrogels are biocompatible surfaces that can be used for a variety of purposes [1–4]. Due to their moisture-rich surfaces and close resemblance to living tissue, hydrogels are used as cell scaffolds [5]. Hydrogels with controllable porosities can be employed for drug delivery [6]. Similar porous hydrogels can also be used as three-dimensional scaffolds to replicate the functions of extra-cellular matrix [7, 8]. Cells grown in such scaffolds can be transferred to target sites for regenerative therapy [9]. Hydrogel scaffolds are useful for the purposes of tissue engineering and vascular engineering [10, 11]. In another example, hydrogel surfaces have also seen use for growth and regeneration of neural cells [12–14]. Specifically, contact lenses used for vision correction are popular medical devices made from hydrogels. Such contact lenses have been attempted as delivery vehicles for stem cells to restore function to damaged eyes [15–18]. The comfort level of contact lenses during usage is dependent on the level of attached proteins from the tear fluid [19]. Therefore, this study focused on creating plasma polymer films that are stable to water exposure and heat sterilization, on the surface of contact lens hydrogel materials. The study also investigated the effects of such films on cell proliferation as well as protein attachment on contact lens surfaces.

Numerous options of chemical precursors are available for the synthesis of hydrogels. These hydrogels are in general considered biocompatible surfaces, but they often require surface treatment to render the surfaces more hospitable for cell adhesion and proliferation. Many elegant methods of surface modification have been described in previous literature reports. While some authors have reported the use of wet chemical treatments to create functional groups on the surfaces of hydrogels, others have used plasma processing methods to generate the desired chemical groups [20–23]. In a previous study, we had pointed out some of the challenges related to surface modification of hydrogels and then demonstrated the creation of some flexible and water-stable plasma polymer films (PPFs) on the surface of methacrylate hydrogels [24].

Various plasma-based methods have been previously described for the surface modification of hydrogels. The easiest one involves exposure of the target substrate to a plasma source, which allows reactive species from the plasma to come in contact with the substrate. This approach has been used in the contact lens industry to render surfaces more hydrophilic and result in increased wearing comfort for users [25]. Another approach combines plasma techniques with wet chemical treatment methods. A plasma source is used to provide reactive species onto the surface of the substrate that is to be modified. Following the exposure to plasma, the substrate is treated with appropriate chemicals that allows desired functional groups to be conjugated with the reactive species that were transferred to the surface from plasma. A simple example of a similar study involved pre-treatment of poly-(methyl methacrylate) (PMMA) with argon (Ar) plasma, following which the treated lenses were dipped in a solution of PEG and/or heparin [26]. A slight modification of the above-described method utilizes wet treatment with chemicals as the first step, followed by treatment using a plasma source. As an example, we can take a study which utilized porous surfaces and exposed them to the chemicals which were to be coated on the porous surfaces. Following this step of pre-treatment with a chemical, the surfaces were subjected to Ar plasma [27]. However, all these methods pale in comparison to the selectivity and efficiency of plasma polymerisation which uses the desired materials to be coated in gaseous form. Such a method eliminates the necessity of solvents and utilises plasma to create fragmentation of the desired coating material. For example, one method used maleic

anhydride and 2-(methylenedioxy) benzene vapours to be plasma polymerised onto the surface of PET. Following this step, the chemical groups were hydrolysed to give rise to reactive COOH groups which were then conjugated with polyethyleneimine via crosslinking reaction [28]. More recent studies have involved plasma polymerisation of gas mixtures utilising ethylene or 1,3-butadiene combined with a heteroatom source in the form of ammonia or carbon dioxide [29, 30].

Most studies in this field point out to the hydrophilicity of the treated surfaces as a key factor in determining the tendency of surfaces to favor cell adhesion and proliferation. In addition, the presence of N-rich groups (primary amine groups specifically) above a minimum critical percentage has also been shown to favor the adhesion and proliferation of cells [31]. Sulfur-rich surfaces have also been studied, and their effect on cell proliferation, differentiation and adhesion has been investigated [32, 33]. Recently, the attachment of proteins and their conformation on the surface has been shown to act as a key step influencing the cell attachment process [34, 35]. These findings are in good agreement with pioneering studies carried out well before the beginning of this century [36]. The above-described plasma polymer films (O-rich, N-rich and S-rich) can not only impart changes to the pristine hydrogel surface in terms of cell proliferation and adhesion but can also be used to covalently immobilize biomolecules of interest [37]. Laminin is one among many biomolecules, and its immobilization on biomaterial surfaces can be used to tune cell adhesion, proliferation as well as migration [38].

In this study, we delve deeper into the material characteristics that influence and control the phenomenon of cell adhesion and proliferation. A low-pressure radio frequency glow discharge system was used to create eight different PPFs on hydrogel surfaces. In addition to surface wettability, chemical composition, and protein attachment quantification, we have studied the conformation of attached proteins on the surface of hydrogels modified with PPFs. Mechanical properties of the PPFs on hydrogels were also investigated and based on this investigation we suggest that wettability is not the key factor influencing cell adhesion and proliferation. Then, immobilization of laminin on the PPFs on hydrogels was carried out, followed by cell culture on the surfaces with immobilized laminin. We finally describe how plasma polymerization could be used to modify hydrogel surfaces with thin PPFs to achieve biomolecule immobilization and control over cell attachment.

Experimental Section

Materials and Methods

Synthesis of Hydrogels

The hydrogels were prepared by UV curing of a liquid monomer. The monomer was a mixture of 2-hydroxyethyl methacrylate, ethylene glycol dimethacrylate and 2-hydroxy-2-methylpropiophenone (supplied by Karrier Medical Materials Co., Ltd., Hsinchu, Taiwan). The monomer is denoted by the term Polymacon and falls in the FDA Group I of low-water, non-ionic polymers. This liquid was shaped into circular discs of 1.12 cm in diameter and 0.15 cm in thickness by placing the liquid inside an aluminium mould of similar dimensions while UV curing. This monomer was a simplified version of a composition that is used in the contact lens industry for manufacture of HEMA copolymer CLs.

Therefore, it is expected to closely mirror the properties of the surface of a commercially available CL.

The liquid monomer was stored in conical centrifuge tubes covered with aluminium foil. As a preparation for the curing step, the monomer was poured into aluminium moulds. The moulds containing the liquid monomer were placed in an enclosure and subjected to UV light (Spectroline, Model XX-15A, USA) for a duration of 30 min. To remove the cured hydrogels from the moulds, they were first washed in a solution of 10% ethanol to remove any excess and unreacted monomer. The washing step was performed for 15 min at 50 °C. After this washing step, the hydrogels were immersed in Type I reverse osmosis water (18 MΩ-cm resistivity) at 50 °C for 16 h. This allowed the hydrogels to expand to their equilibrium swollen state.

Deposition of PPFs on Hydrogels

A low-pressure capacitively coupled RF glow discharge in gas mixtures containing a source of carbon and a source of heteroatom, was used to produce the PPFs on hydrogels. The films were deposited on the circular UV-cured hydrogel discs.

The depositions were performed in a cylindrical stainless-steel vacuum chamber (20 cm in diameter and 50 cm in height) with a disc shaped powered electrode (Ø = 10 cm) on which the samples were placed. A showerhead gas distributor positioned 4 cm above the powered electrode also served as grounded electrode. The chamber was evacuated to a base pressure of ~ 3.5 Pa using a combination of rotary vane for 4.5 min (Pfeiffer DUO 10MC, Germany) and turbomolecular (Pfeiffer TMU 071P, Germany) pump for 2 min. The process mixtures were introduced via mass-flow controllers (see Fig. 1). The gas flow ratio, defined as R = (flow of heteroatom source gas)/(flow of hydrocarbon source gas) was one of the experimental parameters varied to control film composition. Table 1 contains a description of the various experimental parameters used in the present study. The pressure varied from 10 to 80 Pa during deposition runs by a throttling gate valve. An automatic impedance matching network was used to generate the capacitively coupled RF (AEI CESAR

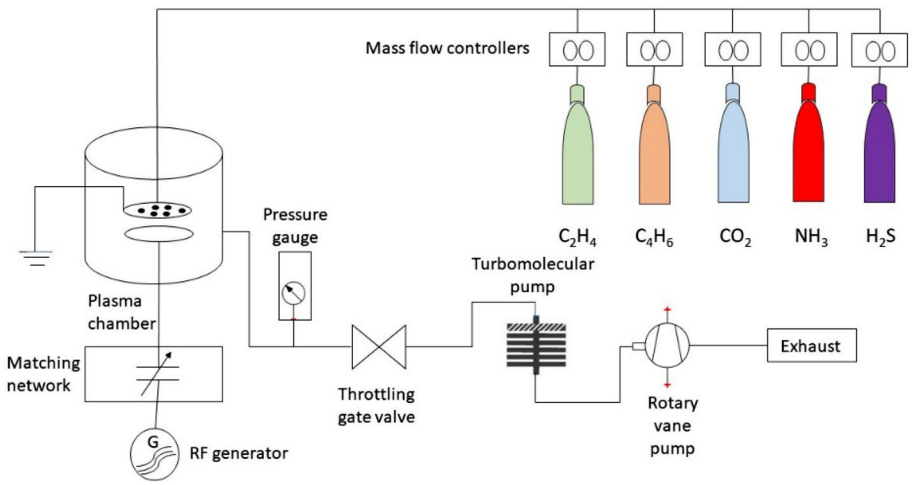

Fig. 1 Schematic drawing of the low-pressure, capacitively coupled RF plasma reactor used for depositing PPFs

Table 1 Plasma treatment conditions on hydrogels

Group name (For ref. in this paper)	Type of PPF	Working pressure (Pa)	Applied RF power (W)	Gas flow conditions (sccm)	Deposition time (minutes)
PPE-Hi	Pure hydrocarbon	10	30	10 sccm C_2H_4	3
PPE-Low	Pure hydrocarbon	80	10	10 sccm C_2H_4	15
PPEN-Hi	Nitrogen-rich	10	30	20 sccm C_2H_4 15 sccm NH_3	10
PPEN-Low	Nitrogen-rich	80	10	20 sccm C_2H_4 15 sccm NH_3	15
PPEO-Hi	Oxygen-rich	10	30	5 sccm C_2H_4 40 sccm CO_2	10
PPEO-Low	Oxygen-rich	80	10	5 sccm C_2H_4 40 sccm CO_2	20
PPES-Hi	Sulfur-rich	10	30	5 sccm C_2H_4 2.5 sccm H_2S	3
PPES-Low	Sulfur-rich	80	10	5 sccm C_2H_4 2.5 sccm H_2S	5

133 13.56 MHz, USA) discharge at power outputs ranging from 10 to 30 W. Deposition times were adjusted according to thickness obtained by stylus profilometry (Bruker Instruments DektakXT, Germany) on PPFs deposited on Si wafers (Data not shown) to obtain a desired minimum thickness (~50–100 nm) of the PPFs on the hydrogels for the cells to be able to interact with. For nanoindentation experiments, deposition times were further increased to obtain at least 500 nm thickness of the coating on silicon wafers.

The deposition of PPFs on hydrogels was done when the samples had not lost all their moisture content and were flexible. There was initially some concern that the water contained in the hydrogels could interfere with the plasma deposition process. However, the hydrogels used are dense and quickly reach a steady state and stop liberating water after they are put under vacuum. This is evidenced by the fact that the vacuum system rapidly reaches base pressure of about 3.5 Pa and that no excess oxygen is incorporated in the deposited films. Treatment conditions involved ethylene as the process gases for the hydrocarbon source, and ammonia/carbon dioxide as the process gases for the heteroatom source. Each type of PPF (Pure hydrocarbon/N-rich/O-rich/S-rich) involved two different sets of process parameters (the lowest and highest values for working pressure and output power) to investigate the effects of these conditions on the cellular response. Before treatment of the hydrogel samples, a blank plasma treatment run would be done to condition the chamber and coat the reactor walls with similar plasma polymer. Before ignition of plasma, the desired gases were allowed to flow for 2–3 min to remove other impurities present in the chamber. At the end of treatment of hydrogel samples, the chamber was cleaned by an etching Ar-O_2 plasma.

Characterization of Surfaces

Surface Chemical Characterization of PPFs on Hydrogels

The plasma reactor is housed inside a MB 200B glovebox, and samples coated with PPFs were placed in the argon atmosphere of the same glovebox till the time of analysis.

Immediately before the analysis (22–24 h after the deposition), samples were transferred to a vacuum transfer module (Thermo Scientific Model no. 831-57-100-2, UK) which enabled samples transfer into the analysis chamber of the XPS instrument (Thermo Scientific K-Alpha, UK) without exposure to air. To maintain a uniform effect of ageing on the samples, XPS analyses were performed within 24–36 h after deposition of the PPFs on the hydrogel samples. Monochromated Al Kα X-rays, producing photons of 1486 eV acquired at take-off angles (TOA) = 0° (normal to the surface) were used for the analyses. Wide scans with step size 1 eV, pass energy 160 eV, dwell time 200 ms and in the range 1200 to − 10 eV were acquired for each sample. The binding energy scale was calibrated with respect to the carbon (C 1 s) peak at binding energy, BE = 284.6 eV. Atomic concentrations were calculated using the Avantage software (Thermo Scientific Version 5.962, UK). A single sample from each plasma condition group was used and three different spots (Spot size = 250 μm) were analysed to get an average atomic composition.

Water Contact Angle Measurements on Hydrogels with PPFs

The static water contact angles of PPFs deposited on hydrogels were measured by using a contact angle goniometer (Future Digital Scientific Corp., NY, USA) connected to a back-lit-camera system and calculating software (SCA 20, DataPhysics Instruments, Germany). The sessile drop method was followed to determine water contact angles of all the samples. A 5 μL droplet of water was dropped onto the PPF-coated hydrogel surface at a rate of 0.5 μL/s. An untreated hydrogel surface was used as a control surface. Measurements were carried out 22–24 h after PPF deposition on the hydrogel at three separate locations on the sample, on a total of four samples for each plasma condition.

Nanoindentation of PPFs on Hydrogels

Experiments were carried out using a hardness tester (Nanovea M1, USA) equipped with a Berkovich three-sided pyramidal indenter (Synton MDP AG, Switzerland). Single repeat indentations at a minimum of five different points on the sample were utilised to calculate hardness and apparent moduli of elasticity. Experimental conditions for the single repeat indentations were initial load—0.03 mN, loading = unloading rate = 0.75 mN/min and peak load = 1 mN. These conditions were chosen to ensure that the depth of indentation was around 10% of the total thickness of the PPF, to avoid substrate effects. For nanoindentation of hydrogels, samples in dry state were used as swollen hydrogels led to tip slippage and errors in force transduction. The PPFs were deposited on flat silicon substrates, instead of hydrogels, to avoid problems caused by roughness of hydrogel, such as tip slippage or area function errors. Data analysis was done according to the Oliver-Pharr method, as described under Appendix A of supplementary material [39].

Sterilization Stability of PPFs on Hydrogels

PPFs were deposited on silicon wafers and sterilization of these PPFs was carried out in a steam sterilization cycle for 15 min at 121 C. After sterilization, the thickness of the PPFs on silicon wafers was measured by contact profilometry (Bruker Instruments, DektakXT, Germany). The thickness of the films after sterilization was then compared to the thickness observed on silicon wafers immediately after deposition to quantify the relative stability of PPFs towards steam sterilization. thickness measurement of the PPFs on hydrogel samples

was not done as the profilometer needle could not get proper readings on the soft, uneven surface of the hydrogel.

Chemical composition of the hydrogels was also studied before and after sterilization to investigate the stability of the PPFs. Two types of XPS scans, survey, and high resolution, were done and compared before and after sterilization. The degree of changes occurring in the chemical composition gave an idea of the relative stability of the PPFs towards steam sterilization.

The high resolution XPS peak analysis was done by first applying a Shirley background. The C1s spectra were fitted with four component peaks (C1–C4) using full-width at half maximum (FWHM) of 1.5 eV. The C1s component's energy and suggested attributions in PPEN and PPEO are shown in Table 2.

Cell Culture Studies

Cell Culture on Hydrogels with PPFs

Rabbit lens epithelial cells (R-LECs, Catalog ID—AG04677, Coriell Institute for Medical Research, USA) were used to study the cellular response to the PPFs on the hydrogels. These cells were chosen for their similarity to human epithelial lens cells and therefore their relevance in a study that explores effect of coatings on contact lens hydrogels. Cells were expanded from frozen stocks in Modified Eagle's Medium (Gibco MEM, NY, USA) supplemented with 10% fetal bovine serum (Gibco FBS, NY, USA), 1% non-essential amino acids (Gibco, NY, USA) and 0.1% penicillin–streptomycin solution. Cells were maintained in T25 flasks in an incubator at 37 °C and 5% CO_2 till they reached 90% confluency. Media was changed every 2nd day, with cells requiring trypsinization on every 5th day.

To study cell attachment on the hydrogels with PPFs, the samples were autoclaved in a cycle of steam sterilization at 121 °C for 15 min. Following the sterilization cycle, the hydrogels with PPFs were placed in the wells of a 24-well plate (Sarstedt Green, Germany) and immersed in 500 uL of phosphate buffered saline (Gibco DPBS, NY, USA) and placed in the incubator for the purpose of equilibration. On the next day, the wells were emptied of the PBS, and R-LECs were seeded on the surfaces at a density of 200,000 cells/well. This cell density was chosen after iterative optimization involving various cell numbers (10,000 cells/well, 20,000 cells/well, 50,000 cells/well, 100,000 cells/well and 200,000 cells/well). The final cell density was chosen because it allowed proper examination via optical imaging and also enabled quantification by WST-8 assay. These cells were then allowed to grow on the surface

Table 2 Typical attributions of C1s peak fit components of nitrogen rich and oxygen rich plasma polymer films

Peak label	Possible chemical bonds	PPE:N Peak BE (eV)	Possible chemical bonds	PPE:O Peak BE (eV)
C1	C–C, C=C	284.32	C–C, C=C	284.32
C2	C–N, C=N, C–C: N	C1 + 0.56	C–OR (COH, COC)	C1 + 1.29
C3	C: N, C–O–C=O	C1 + 1.54	C=O	C1 + 2.34
C4	N–C–O, N–C=O, C=O	C1 + 2.61	COOR (O=C–OH, O=C–OC)	C1 + 4.10

of the hydrogels for 48 h. At the end of 48 h, the hydrogel samples with the R-LECs on the surface were transferred to another 24-well plate with PBS in its' wells for the purpose of rinsing. After gently immersing the hydrogels with R-LECs in the PBS-filled wells, the PBS was removed from the wells and 500 µL solution of 10% WST-8 reagent in MEM was added to each of the wells. A control group of cells on untreated hydrogel surfaces was included.

After 4 h of incubation of the WST-8 (ApexBio CCK-8, USA) reagent, the absorbance of the solution at 450 nm was measured in a spectrophotometer (Bio-Rad xMark, USA) to get an estimate of the relative quantities of cells that had attached to each hydrogel sample. Images of the cells on the hydrogel samples were also captured using an optical microscope (VWR Professional Plus, USA) to qualitatively compare cell attachment across various surfaces.

Relative cell attachment was calculated according to the following formula:

$$\frac{\left(Absorbance_{Sample} - Absorbance_{Blank}\right)}{\left(Absorbance_{Control} - Absorbance_{Blank}\right)} \times 100 \quad (1)$$

The wells containing hydrogel samples with different PPFs were "samples" and the wells containing untreated hydrogel samples were "control". Wells with just MEM were taken as "blanks."

Protein Attachment Studies on Hydrogels with PPFs

Bovine serum albumin (Sigma Aldrich BSA, USA) was used in this study because of its resemblance to albumin, a key component of the human tear fluid that lubricates the microenvironment of the eye.

Two types of experiments were carried out to investigate the response of the PPFs to proteins in solution. The first one involved quantification of amount of proteins getting adsorbed onto the surface of the PPFs after incubation in protein solutions (40 mg/mL for BSA) for 24 h at standard ambient temperature. Quantification was carried out according a method based on ATR-FTIR described by Castillo et al. [40]. Briefly, the amide I band (1600–1720 cm^{-1}) of the ATR-FTIR absorption spectra (Bruker Instruments Nicolet IS50, Germany) were used to get a relative estimate of the proteins getting adsorbed onto the surfaces of PPFs compared to untreated hydrogel surfaces. Scans of untreated hydrogels were measured and taken as baselines for the rest of the samples with PPFs on surface of the hydrogels.

In the second study, the amide I peak was deconvoluted by a peak fitting method to get an idea of the various conformations of the proteins after they had been adsorbed onto the PPFs [41]. Four conformational structures of the proteins were assumed: coils (peak centered at 1675 cm^{-1}), α-helix (peak centered at 1655 cm^{-1}), β-sheets (peak centered at 1618 cm^{-1}) and a random statistical distribution of other structures (peak centered at 1635 cm^{-1}). Peaks were fit after taking a linear baseline from 1600 to 1720 cm^{-1} and then fit by peak resolve function using Gaussian–Lorentzian fit algorithms inbuilt in OMNIC software (Bruker Instruments, Germany).

Laminin Immobilization Studies

Laminin from mouse Engelbreth-Holm-Swarm (EHS) sarcoma (Product code: 11,243,217,001, Sigma Aldrich, USA) was utilized for the immobilization studies on hydrogel samples with plasma polymer films. Laminin stock solution of 100 ug/mL was prepared under sterile conditions by diluting the product (as received) with phosphate

buffered saline. This stock solution was stored at 4 °C for about 1–2 months, and it was diluted to a final concentration of 4 ug/mL with phosphate buffered saline for the immobilization experiments.

Quantification of Laminin Immobilization

Hydrogels with PPFs were placed in the wells of a 24-well plate (Sarstedt Green, Germany) and immersed in 500 uL of 4 ug/mL laminin in phosphate buffered saline and then placed in the incubator for 22–24 h at a temperature of 37 °C and 5% CO_2 the purpose of equilibration. After equilibration, the hydrogels were taken out of the solution and placed inside the argon atmosphere of the MB200B glovebox for another 22–24 h for the purpose of drying and degassing. Following this, XPS analyses were carried out in a Thermo Scientific K-Alpha instrument, according to the methods described in "Surface Chemical Characterization of PPFs on Hydrogels" section. Atomic concentrations were calculated using the Avantage software (Version 5.962).

The total atomic composition of nitrogen on the hydrogel surfaces was used as a measure of the amount of laminin immobilized on the surface of the samples. A sample of hydrogel immersed in phosphate buffered saline and another hydrogel without any plasma treatment immersed in laminin were used as controls.

Cell Culture on Hydrogel Surfaces After Laminin Immobilization

Hydrogel samples with PPFs were autoclaved in a cycle of steam sterilisation at 121 °C for 15 min. As described in "Quantification of Laminin Immobilization" section, these samples were placed in the wells of a 24-well plate (Sarstedt Green, Germany) and immersed in 500 uL of 4 ug/mL laminin in phosphate buffered saline and then placed in the incubator for 22–24 h at a temperature of 37 °C and 5% CO_2 the purpose of equilibration. To study cell attachment, these samples were then placed in the wells of a new 24-well plate and R-LECs were seeded on the surfaces at a density of 200,000 cells/well. These cells were then allowed to grow on the surface of the hydrogels for 48 h. At the end of 48 h, the hydrogel samples with the R-LECs on the surface were transferred to another 24-well and WST-reagent was used to evaluate cell proliferation of the surfaces (according to the methods described in "Cell Culture on Hydrogels with PPFs" section). A control group of cells on untreated hydrogel surfaces immersed in PBS, and untreated hydrogel surface immersed in laminin were included as controls.

Results

Surface Chemical Characterization of PPFs on Hydrogels

The surface of untreated hydrogel showed the presence of carbon and oxygen functionalities (Table 3). The amount of carbon was higher in the hydrocarbon-rich PPE-High and PPE-Low films. Increased nitrogen incorporation was shown in the PPEN-High and PPEN-Low films. While the total atomic composition of the untreated hydrogel and oxygen-rich films (PPEO-High and PPEO-Low) was statistically indistinguishable, the process of plasma polymerization introduced different chemical groups onto the surface of

PPEO-High and PPEO-Low films (Table 3). This was evidenced from the high resolution XPS scans.

Increased amount of sulfur was detected in both PPES-High and PPES-Low films. Slight amount of oxygen incorporation was also detected in both S-rich films, like N-rich films (Table 3).

Water Contact Angle Measurements on Hydrogels with PPFs

Water contact angles of untreated hydrogels and hydrogels with different PPFs are shown in Fig. 2. Hydrogels used in this study were composed primarily of methacrylate, and these were not very hydrophilic in nature. In the contact lens industry, hydrophilic compounds such as N-vinyl-2-pyrrolidone are used as additives to make the surface of contact lens hydrophilic. This study, however, avoided these additives as they would make the chemical characterization difficult and the plasma polymerization process more complicated. The hydrogels with PPE-High and PPE-Low also display similar water contact angles, due to their pure hydrocarbon nature. Addition of polar moieties to the hydrocarbon chains can bring down the water contact angle, and therefore we see lower figures on both O-rich, N-rich and the S-rich groups. Difference observed in the sub-groups of each type of PPF could be explained by the differences in the chemical groups observed on the surface.

For example, XPS survey scans show that the chemical composition of PPEO-High and PPEO-Low are identical (Table 3). However, HR-XPS scans provide more information into the proportion of chemical groups on the surface of PPEO-High and PPEO-Low (Table 6a). These differences could contribute to the variations observed in WCA even though the survey scan results seem identical. PPES-Low and PPES-High have quite different surface chemical compositions, and therefore show different WCAs.

Nanoindentation of PPFs on Hydrogels

All the PPFs displayed higher elastic modulus and hardness compared to the untreated hydrogel surface (Table 4). For pure hydrocarbon PPFs, there was a clear difference between PPE-High and PPE-Low. PPE-High was stiffer than PPE-Low, but this trend was reversed in the O-rich, N-rich and S-rich PPFs. PPEO-High, PPEN-High, and

Table 3 Surface atomic composition of hydrogel samples; data is expressed as mean ± standard deviation of at least 3 measurements

	Carbon (%)	Oxygen (%)	Nitrogen (%)	Sulfur (%)
Untreated hydrogel	69.7 ± 1.5	30.3 ± 1.2	Undetected	Undetected
PPE-Hi	97.3 ± 1.3	2.7 ± 0.5	Undetected	Undetected
PPE-Low	98.7 ± 1.5	1.3 ± 0.2	Undetected	Undetected
PPEO-Hi	71.2 ± 1.1	28.8 ± 0.7	Undetected	Undetected
PPEO-Low	74.2 ± 2.9	25.8 ± 1.5	Undetected	Undetected
PPEN-Hi	83.6 ± 0.9	1.7 ± 0.4	14.7 ± 0.6	Undetected
PPEN-Low	84.1 ± 2.8	1.0 ± 0.6	14.9 ± 0.2	Undetected
PPES-Hi	84.4 ± 0.5	2.9 ± 0.5	Undetected	11.5 ± 0.3
PPES-Low	79.2 ± 0.1	1.9 ± 0.2	Undetected	18.9 ± 0.2

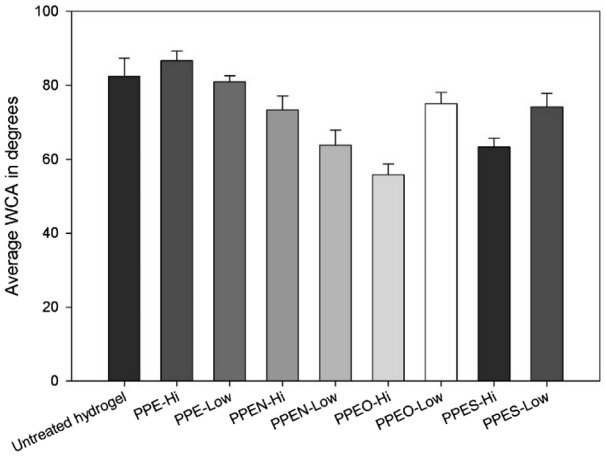

Fig. 2 Water contact angles of different hydrogel samples with PPFs

PPES-High showed lower stiffness compared to both PPEO-Low, PPEN-Low and PPES-Low respectively.

The H/E ratio for the samples reflected a trend like the elastic modulus and hardness data for PPEO and PPEN samples but it was reversed in the case of PPES samples. All the PPFs displayed higher elastic strain threshold to failure compared to an untreated hydrogel surface. All nanoindentation studies were performed on samples directly after plasma deposition on silicon wafers (Table 5).

Sterilization Stability of PPFs on Hydrogels

Stability of the PPFs was evaluated by comparing the thickness of PPFs on a profilometer before and after steam sterilization. All the PPFs on hydrogel surfaces showed durability towards the steam sterilization process (Fig. 3). The PPFs named PPEO-High, PPEO Low

Table 4 Mechanical properties of hydrogel samples derived from nanoindentation tests

	Apparent elastic modulus, E_s (In GPa)	Nanoindentation hardness, H (In GPa)	H/E (Elastic strain to failure)
Untreated hydrogel	2.6 ± 1.7	0.1 ± 0.1	0.1 ± 0.1
PPE-Hi	43.5 ± 11.0	6.2 ± 1.9	0.2 ± 0.1
PPE-Low	12.6 ± 4.3	0.8 ± 0.3	0.1 ± 0.1
PPEO-Hi	27.2 ± 8.7	8.5 ± 3.7	0.3 ± 0.1
PPEO-Low	38.2 ± 4.2	3.5 ± 1.4	0.1 ± 0.1
PPEN-Hi	28.6 ± 6.7	10.4 ± 6.5	0.3 ± 0.1
PPEN-Low	61.5 ± 18.0	16.0 ± 7.3	0.3 ± 0.1
PPES-Hi	53.9 ± 14.2	6.3 ± 1.8	0.1 ± 0.1
PPES-Low	77.9 ± 9.1	15.4 ± 2.6	0.2 ± 0.1

Data is expressed as mean ± standard deviation of at least 5 measurements

Table 5 Surface atomic composition of hydrogel samples before and after sterilization; data is expressed as mean ± standard deviation of at least 3 measurements; N/A means the element of concern was undetectable

	Before sterilization				After sterilization			
	C%	O%	N%	S%	C%	O%	N%	S%
PPE-Hi	97.3 ± 1.3	2.7 ± 0.5	N/A	N/A	93.1 ± 1.1	6.9 ± 0.6	N/A	N/A
PPE-Low	98.7 ± 1.5	1.2 ± 0.2	N/A	N/A	95.0 ± 1.2	3.1 ± 0.8	N/A	N/A
PPEO-Hi	71.2 ± 1.1	28.8 ± 0.7	N/A	N/A	67.7 ± 0.9	32.2 ± 1.0	N/A	N/A
PPEO-Low	74.2 ± 2.9	25.8 ± 1.5	N/A	N/A	76.4 ± 0.8	23.6 ± 1.4	N/A	N/A
PPEN-Hi	83.6 ± 0.9	1.7 ± 0.4	14.7 ± 0.6	N/A	78.4 ± 2.3	12.8 ± 0.7	7.7 ± 0.5	N/A
PPEN-Low	83.9 ± 2.8	1.1 ± 0.6	14.9 ± 0.2	N/A	78.6 ± 1.3	14.3 ± 0.6	7.2 ± 0.4	N/A
PPES-Hi	84.4 ± 0.5	2.9 ± 0.5	N/A	11.5 ± 0.3	83.3 ± 0.1	7.1 ± 0.3	N/A	9.5 ± 0.1
PPES-Low	79.2 ± 0.1	1.9 ± 0.2	N/A	18.9 ± 0.2	80.6 ± 0.8	2.1 ± 0.1	N/A	17.3 ± 0.7

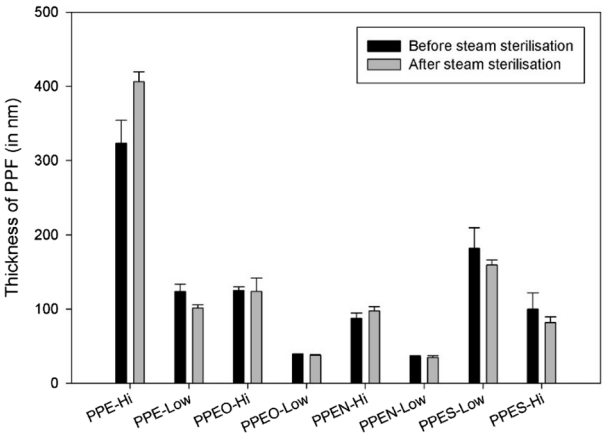

Fig. 3 Thickness of PPFs measured by profilometry before and after sterilization; data is expressed as mean ± standard error of at least 3 measurements

and PPEN-Low showed negligible changes in thickness before and after steam sterilization. PPEN-High showed a slight increase, whereas PPE-Low, PPES-Low and PPES-High showed a slight decrease in thickness. The most notable change was the swelling recorded in the PPE-High films after sterilization.

The hydrogel samples on their own are very stable towards sterilization and displayed no changes in structure after sterilization. However, thickness changes of PPFs on hydrogel samples were difficult to measure because of the softness and the uneven nature of the sample surfaces.

All the samples reported an increase in the quantity of oxygen-rich chemical groups after autoclaving (Fig. 4). For the hydrocarbon-rich PPFs (PPE-High and PPE-Low), the samples were almost devoid of oxygen-rich chemical groups prior to sterilization, but showed presence of C–O, C=O and COOR groups after sterilization (Table 6a). In the oxygen-rich PPFs (PPEO-High and PPEO-Low), O-rich chemical groups were present on the surface after plasma polymerization. In the PPEO-High sample, there was an increase in the proportion of chemical groups containing C=O bonds after autoclaving (Table 6a). However, in the case of PPEO-Low samples, there was a decrease in the proportion of

COOR groups. As discussed earlier, this could be attributed to the hydrolysis and subsequent dissolution of high molecular weight oligomeric O-rich chains.

The amount of N-rich chemical groups in PPEN-High and PPEN-Low samples decreased after sterilization, while there was introduction of O-rich chemical groups (C=O) in both the samples after sterilization (Table 6b). This observation was consistent with the decrease in total amount of nitrogen content from XPS survey scans (Table 5). Similarly, the amount of S-rich chemical groups in PPES-High and PPES-Low showed a decrease after sterilization. Interestingly, a higher proportion of O-rich chemical groups were introduced to PPES-High samples after sterilization, compared to PPES-Low samples. This shows that PPES-Low is one of the best performing samples, in terms of resistance to sterilization.

Cell Culture on Hydrogels with PPFs

Results of the cell adhesion studies on hydrogels with different PPFs are shown in Figs. 5 and 6. The R-LECs showed a mixed response to the surface of an untreated hydrogel (Fig. 5c), with some cells exhibiting rounded morphologies and the rest showing signs of spreading and attachment. In the case of hydrogels with pure ethylene PPFs, R-LECs showed no signs of attachment after 48 h of incubation. Both the sample groups were devoid of any attachment throughout the whole surface (Fig. 5a, b).

In comparison, the R-LECs showed a favorable response to the oxygen-rich PPFs on the hydrogels. In both the sample groups (Fig. 5d, e), cells showed increased attachment relative to the surface of an untreated hydrogel control. The morphology of cells on the O-rich PPFs was radically different from that of cells on untreated hydrogels. No signs of detachment (rounded, floating cells) were visible, and all the cells exhibited spreading on the surface.

However, in the case of nitrogen-rich PPFs, the R-LECs showed preferential attachment to one sample group over the other (Fig. 5f, g). R-LECs favored the hydrogel with PPEN-Low, with signs of good attachment and spreading (Fig. 5g). But on the hydrogel with PPEN-High, there were no cells at all (Fig. 5f). The untreated hydrogel control displayed lower attachment and proliferation of R-LECs compared to PPEN-Low.

The R-LECs showed the maximum preference in attachment to sulfur-rich PPFs, across all samples tested. Preferential attachment was shown to the PPES-Low sample (Fig. 5i), over PPES-Hi sample (Fig. 5h). However, the level of cell attachment on PPES-Hi sample was almost equal to that of the highest attachments seen on PPEO-High, PPEO-Low and PPEN-Low. The cell attachment displayed on PPES-Low was almost 3 × that of the highest levels seen on any other sample.

The observations made from optical microscopy images were confirmed by cell viability tests employing WST-8 reagent. WST-8 reagent is a highly water-soluble tetrazolium salt [2-(2-methoxy-4-nitrophenyl)-3-(4-nitrophenyl)-5-(2,4-disulfophenyl)-2H-tetrazolium, monosodium salt] which produces a water-soluble formazan dye (absorbance 450 nm) upon reduction (by dehydrogenases abundant in viable cells) in the presence of an electron mediator, similar to the popular MTT assay. In Fig. 6, the relative viability (compared to an untreated hydrogel surface) of cells on hydrogels with different PPFs is shown. Cell attachment on pure ethylene PPFs was lower than an untreated hydrogel. While almost no cells were spotted on both these surfaces in the optical microscopy images, the slightly higher absorbance of PPE-High at 450 nm could be attributed to the dark-brownish color imparted

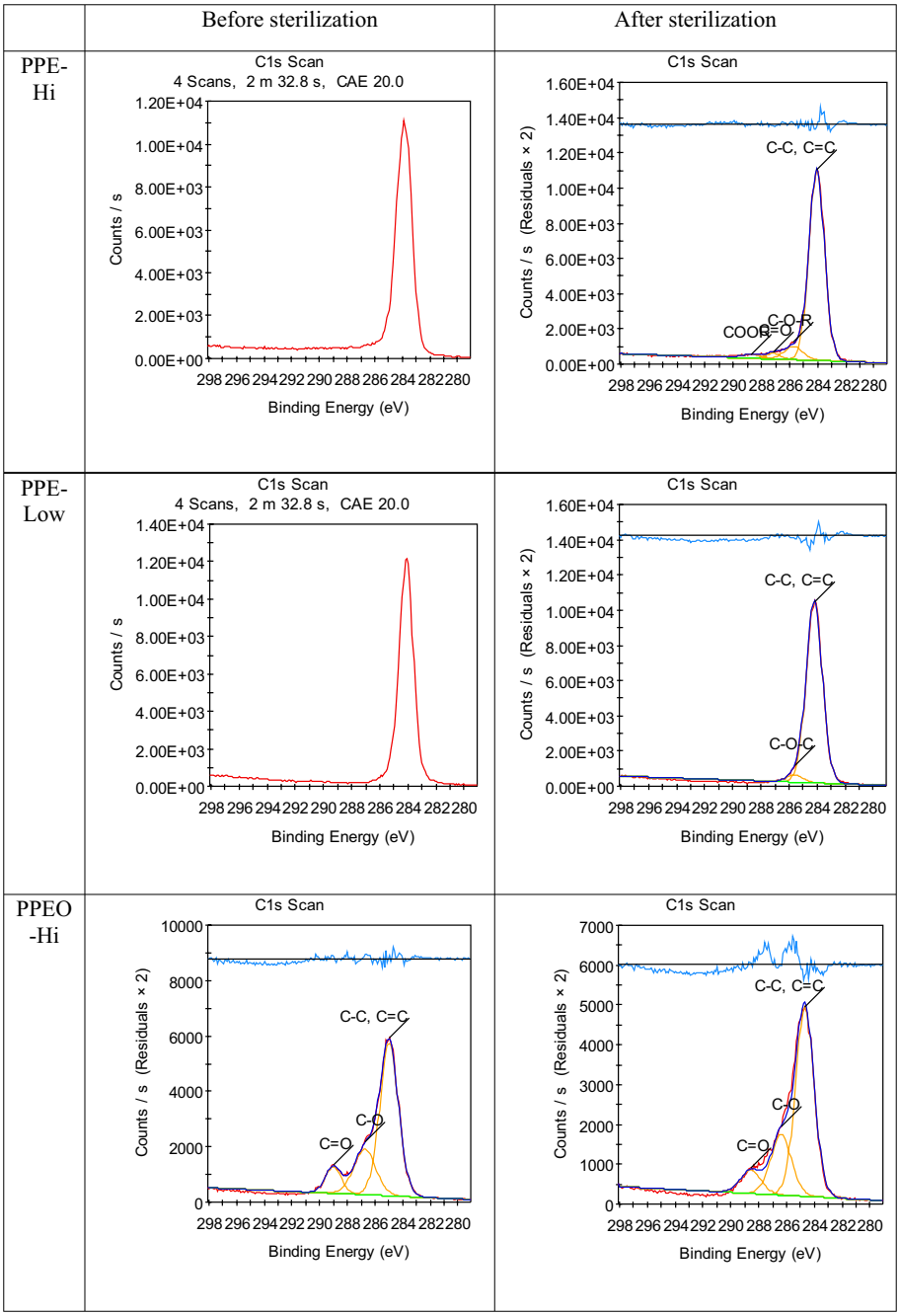

Fig. 4 Changes in chemical composition of the plasma polymer films on hydrogel samples after sterilization as demonstrated by high-resolution XPS

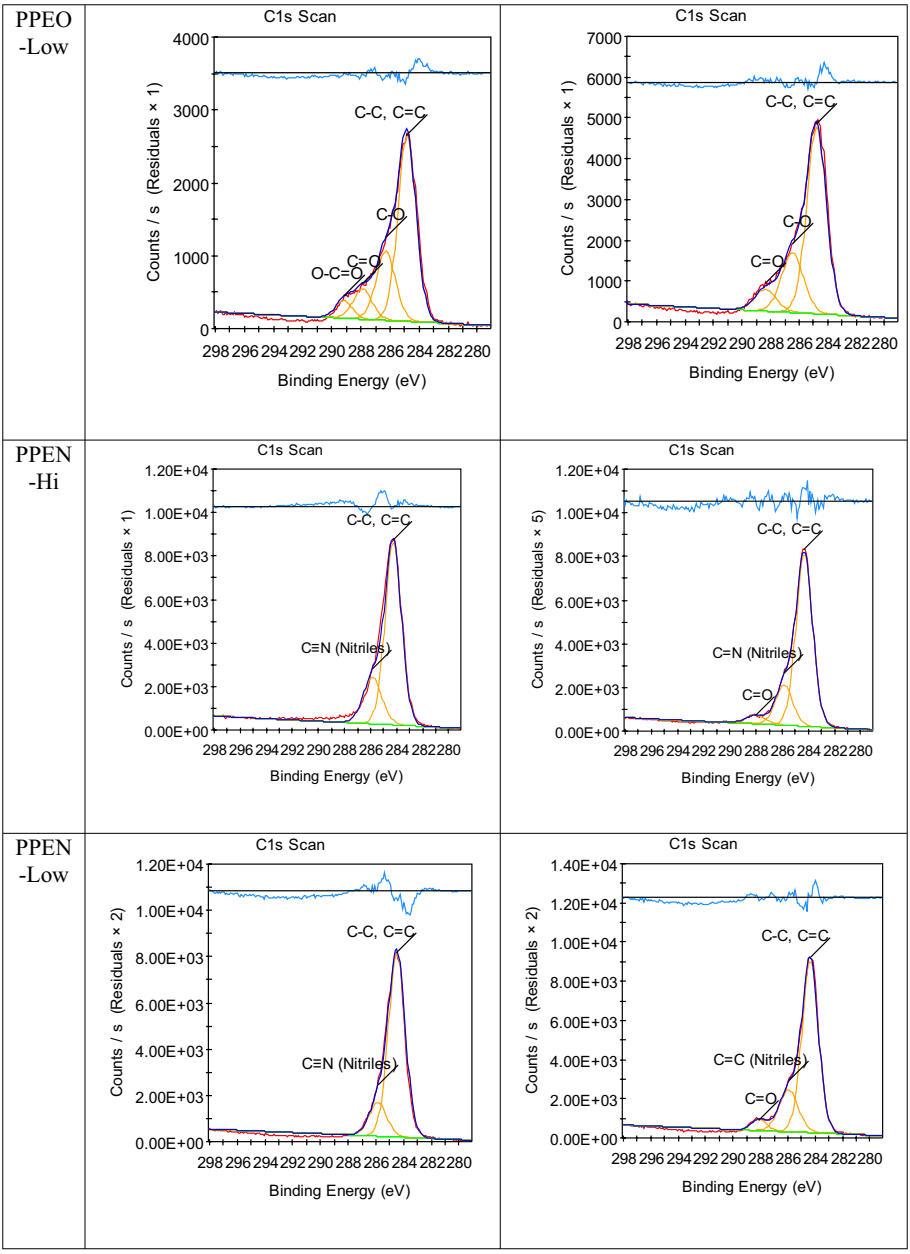

Fig. 4 (continued)

onto the hydrogel due to the PPF formation. On the other hand, the sample with PPE-Low was clear and transparent.

Both the oxygen-rich PPFs showed similar levels of relative viability of R-LECs. Again, the slightly higher absorbance at 450 nm could be attributed to the darker color of the

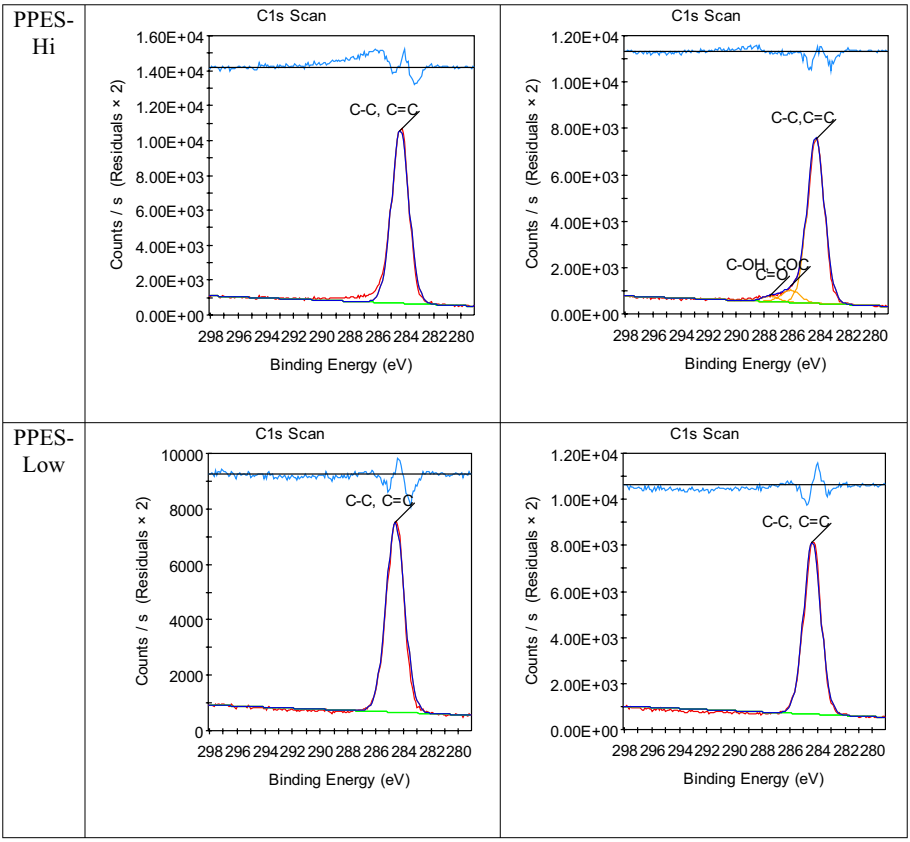

Fig. 4 (continued)

PPEO-High film formed at higher power and lower pressure. The film PPEO-Low was formed at a lower power and higher pressure and was transparent. In agreement with the optical microscopy images, PPEN-High showed exceptionally low relative viability of R-LECs whereas PPEN-High displayed almost 1.5 × viability of R-LECs relative to an untreated hydrogel.

Protein Adsorption Studies on Hydrogels with PPFs

BSA is a large protein with a molecular weight of 66 kDa, with a net negative charge. BSA displayed strong adsorption to PPEN-Low films (Fig. 7a). Adsorption of BSA to PPEN-Low was twice the adsorption to PPEO-Low and PPE-Low films. BSA adsorption levels were similar on PPEO-High and PPEN-High films. In comparison, PPE-High showed slightly lesser level of BSA adsorption.

BSA is a major component of the media used for cell culture, as the media itself contains proteins and is further supplemented with fetal bovine serum. Deconvolution of the amide I peak (1600–1700 cm^{-1}) of BSA adsorbed on the hydrogels gave an estimate of the relative proportions of the conformational states (Fig. 7b). The BSA adsorbed on the untreated hydrogel and the hydrocarbon-rich films (PPE-High and PPE-Low) showed

Table 6 Results of high resolution C1s XPS scans showing changes in chemical composition of (a) pure hydrocarbon/O-rich PPFs before and after sterilization (b) N-rich PPFs before and after sterilization (c) S-rich PPFs before and after autoclave

(a) Pure hydrocarbon/O-rich PPFs before and after sterilization

	Before autoclave				After autoclave			
Chemical groups	C–C, C=C	C–O–R	C=O	COOR	C–C, C=C	C–O–R	C=O	COOR
PPE-Hi	~ 100.0	0.0	0.0	0.0	87.6	7.5	2.5	2.4
PPE-Low	~ 100.0	0.0	0.0	0.0	96.2	3.8	0.0	0.0
PPEO-Hi	66.8	23.5	9.9	0.0	66.5	24.0	9.6	0.0
PPEO-Low	68.5	18.4	8.7	4.5	67.0	24.2	8.9	0.0

(b) N-rich PPFs before and after sterilization

	Before autoclave			After autoclave		
Chemical groups	C–C, C=C	C=N	C=O	C–C, C=C	C=N	C=O
PPEN-Hi	77.8	22.2	0.0	76.5	18.7	4.8
PPEN-Low	84.0	16.0	0.0	74.3	21.2	4.5

(c) S-rich PPFs before and after autoclave

	Before autoclave			After autoclave		
Chemical groups	C–C, C=C	C–O–R	C=O	C–C, C=C	C–O–R	C=O
PPES-Hi	100.0	0.0	0.0	89.8	7.2	3.0
PPES-Low	100.0	0.0	0.0	100.0	0.0	0.0

similar proportions of beta-sheets, non-ordered structures, alpha-helices, and coils. In the case of PPEO-High, BSA showed a slight increase in the conformational state of alpha-helices, and a decrease in the state of coils. The opposite effect was observed in the PPEO-Low films, accompanied by a slight increase in the proportion of beta-sheets (Only sample to do so). A similar trend was observed in the N-rich films, with an increase in alpha-helices in the PPEN-High and an increase in the coils in PPEN-Low.

A very different trend was observed in the PPES samples. Both the PPES samples displayed an increased proportion of beta-sheets, with the PPES-Low having a higher proportion of beta-sheets than PPES-High. The proportion of alpha-helices and non-ordered structures was reduced in the PPES samples, compared to others. The proportion of coils remained unchanged compared to that on an untreated hydrogel surface.

Laminin Immobilization on Hydrogel Samples and Cell Proliferation on Laminin-Immobilized Surfaces

The amount of nitrogen on the surface of hydrogel samples was used as an indirect measure of immobilized laminin, based on a method developed by Raquez et al. A piece of pure hydrogel immersed in PBS showed no signals of N1s, as the methacrylate hydrogels used in this study lack any nitrogen chemical groups. However, the surface of an untreated hydrogel immersed in laminin showed the presence of nitrogen (2nd bar, Fig. 8). This shows that there is some non-specific binding of laminin to an untreated hydrogel surface. However,

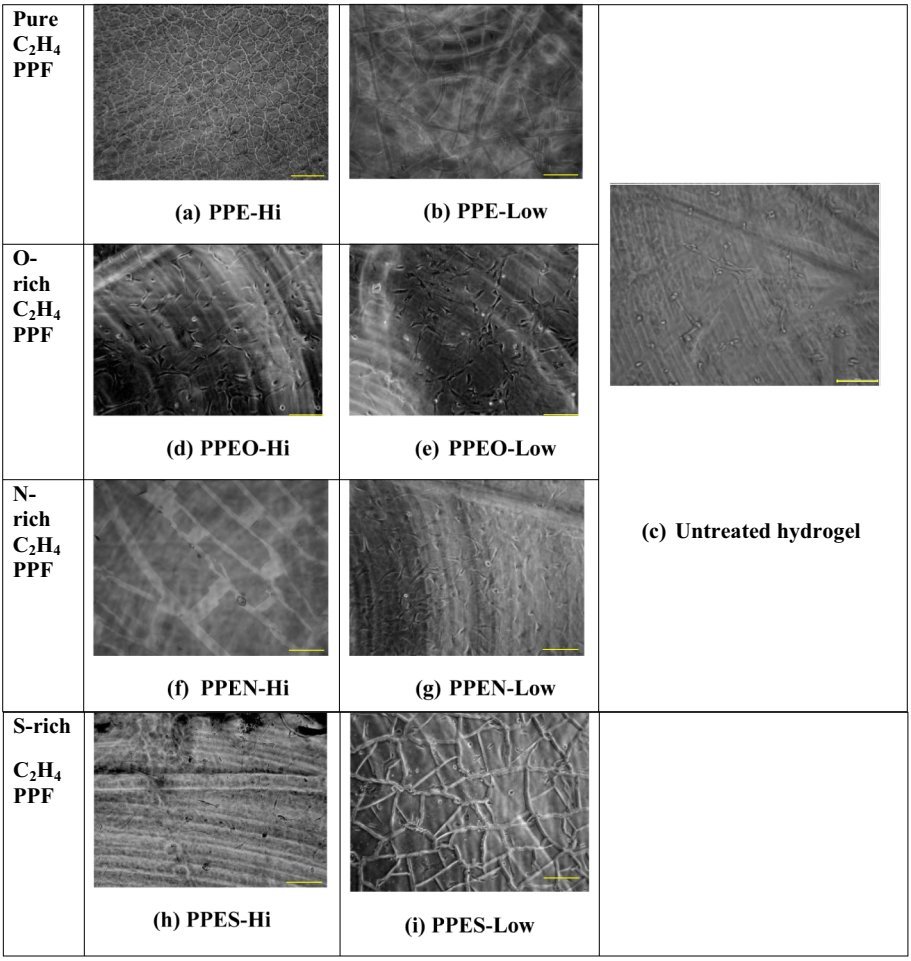

Fig. 5 Optical microscopy images of R-LECs on different hydrogel samples with C_2H_4 PPFs at the end of 48 h of incubation (Scale bar = 200 µm)

this amount is among the lowest values displayed (at par with PPEN-High and PPEN-Low) which shows that N-rich surfaces do not enhance laminin immobilization. O-rich surfaces (PPEO-High and PPEO-Low) provided a slight increase in laminin immobilization compared to untreated hydrogel surfaces. The maximum amount of laminin immobilization was observed in PPES surfaces, with both PPES-High and PPES-Low showing at least 2 × the amount of immobilization on untreated hydrogel surfaces.

Since PPES samples displayed the highest amount of laminin immobilization, these samples were used for further evaluation of cell attachment (Fig. 9). In each of the cases, immobilization of laminin led to a significant increase in the cell attachment compared to a similar surface without laminin immobilization. In the case of PPES-High, the increase in cell attachment after immobilization of laminin was 4.74 × that of a pure PPES-High surface. Similarly, for PPES-Low, the increase recorded after immobilization was 2.18 × that of a pure PPES-Low surface.

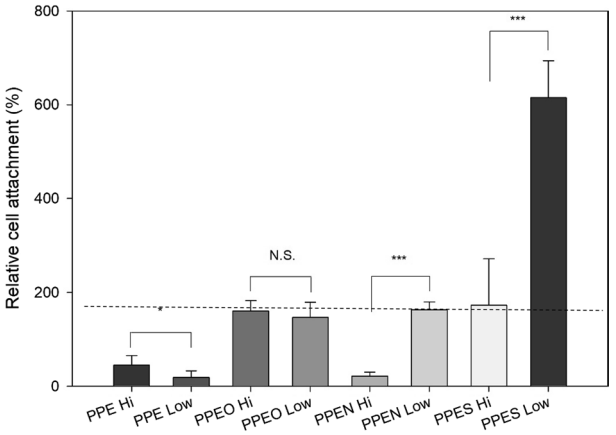

Fig. 6 Relative cell attachments calculated from absorbance values at 450 nm after WST-8 incubation for different hydrogel samples with C_2H_4 PPFs relative to an untreated hydrogel sample denoted by dashed line (Data presented as mean and error bars represent S.D., *denotes $p < 0.1$ and *** enotes $p < 0.05$ and N.S. denotes statistical non-significance

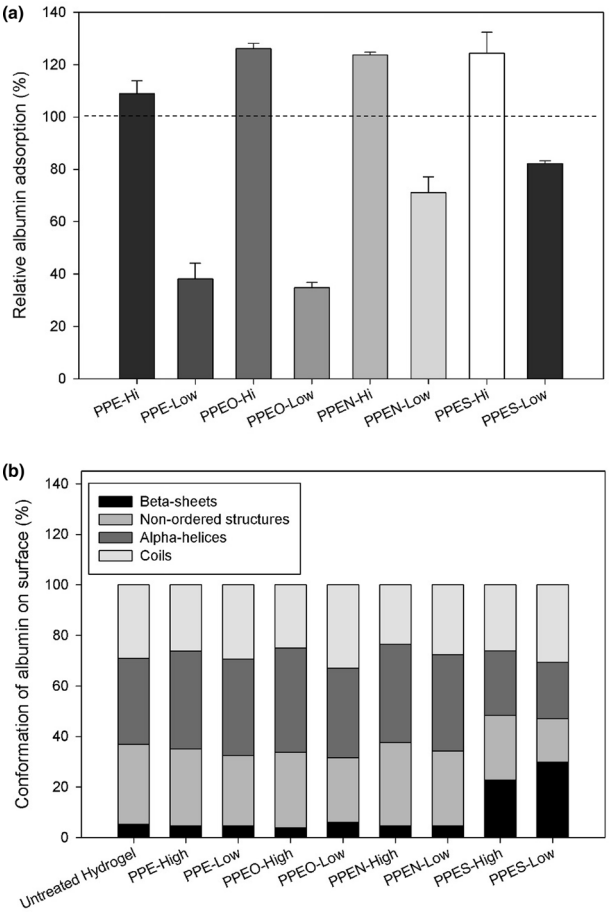

Fig. 7 **a** Relative BSA adsorption on different hydrogel samples with PPFs relative to an untreated hydrogel sample denoted by dashed line. **b** Conformational state of BSA on the surface of untreated hydrogel and different PPFs

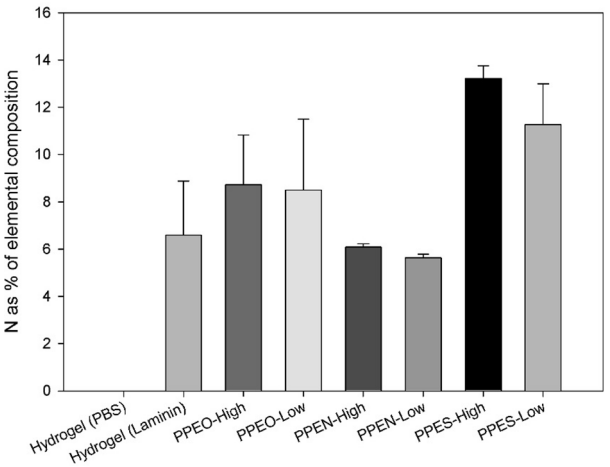

Fig. 8 Atomic nitrogen as % of total surface atomic composition for hydrogel samples with PPFs after laminin immobilization by dip coating

Optical microscopy images showed that cells preferentially attached themselves to PPES-Low surfaces with laminin immobilized (Fig. 10b) on the surface. PPES-High with laminin immobilized (Fig. 10a) displayed a lower number of cells attached onto it, however both the surfaces were higher compared to an untreated hydrogel surface (Fig. 10c).

Discussion

Control of cell attachment on hydrogels is a key element to their use as scaffolds for cell and tissue engineering. Change of synthesis protocol to modify the chemical composition of the hydrogel is possible but could lead to undesirable changes in the bulk properties of the hydrogel. Creation of a thin organic layer on the hydrogel surface by plasma polymerization is an attractive alternative as cells interact with the top few nanometers, and this organic layer would not affect the bulk properties of the hydrogel. The thin organic layer can also be used to covalently immobilize desirable biomolecules (e.g., Laminin) on the

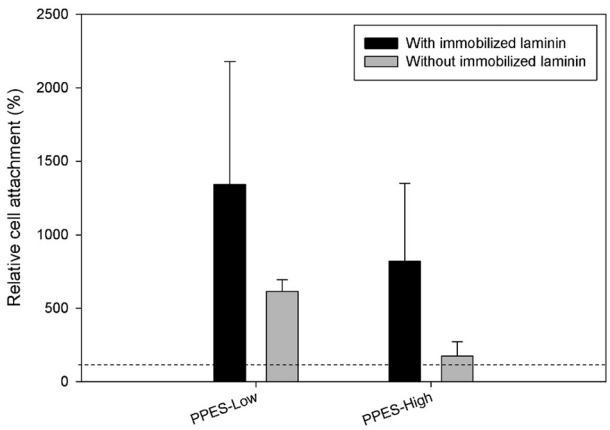

Fig. 9 Relative cell attachments calculated from absorbance values at 450 nm after WST-8 incubation for PPES samples with and without immobilized laminin on surface; relative to an untreated hydrogel sample denoted by dashed line

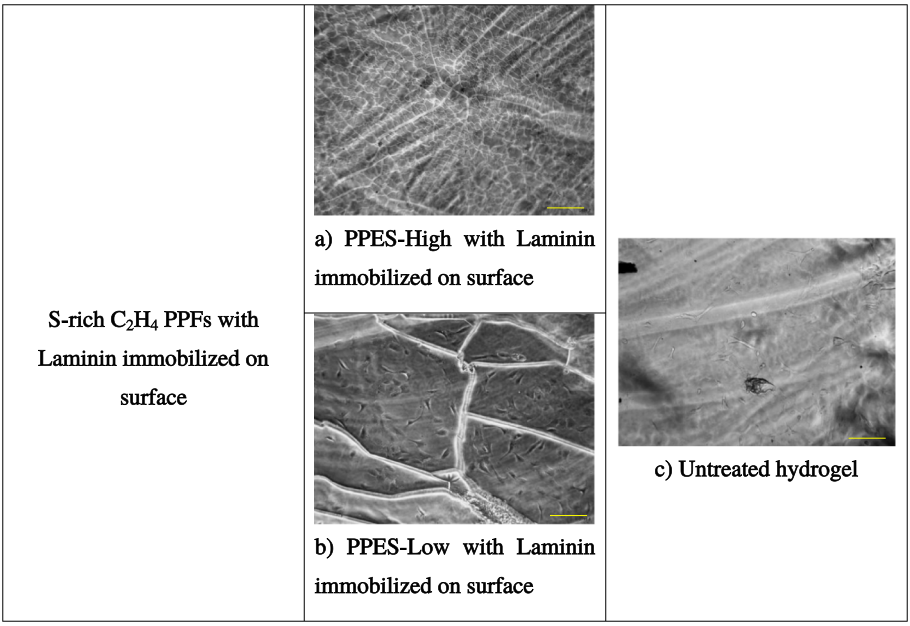

Fig. 10 Optical microscopy images of R-LECs on PPES samples with immobilized laminin on surface at the end of 48 h of incubation (Scale bar = 200 µm)

hydrogel surface. Additionally, plasma polymerization has the advantage of being a solvent free process and therefore does not create undesirable effects in the bulk hydrogel matrix.

The primary goal of the study was to understand how plasma processing conditions affect the behaviour of water-stable plasma polymer films on hydrogel surfaces with the aim of influencing cell proliferation and protein adsorption, so that such surface modified contact lenses could be examined for the purpose of cell delivery. Nitrogen and oxygen-rich functional groups are well studied for their ability to influence cell adhesion. However, the effect of different plasma parameters to give rise to differing nitrogen and oxygen-rich chemical groups hasn't been studied. Similarly, the effect of sulfur-rich chemical groups on cell attachment on hydrogels has been studied in lesser detail compared to nitrogen and oxygen-rich chemical groups. Each of these chemical groups would also influence protein adsorption, which would also influence cell proliferation. To a lesser extent, these surfaces would play a role in the mechanical properties experienced by the cells, as most plasma polymerised surfaces are denser and stiffer compared to hydrogels. These reasons, in addition to the ability of enabling covalent attachment of biomolecules, were why the said chemical groups were chosen for incorporation onto hydrogel surfaces.

Such hydrogel scaffolds must be sterilized before being seeded with cells. To ensure optimum functionality, the PPFs on the surface of hydrogels should not display any thickness changes or delamination after the sterilization process (Fig. 3). The eight samples used in this study did not display any structural changes after sterilization. The PPFs on the hydrogels did not display any signs of delamination and this ensured validation of a key step in the biomedical device usage cycle. Preliminary validation of the delamination resistance of the hydrogels was validated in an earlier publication [23]. Visual examination revealed no changes on the plasma polymer films, and profilometry measurements

displayed no major reduction in coating thicknesses after wet heat sterilization (Fig. 3). Some chemical changes were observed in the PPFs on hydrogels after sterilization. The O/C ratio of PPE-High and PPE-Low surfaces increased from 0.03 to 0.07, and 0.01 to 0.03, respectively. Similarly, the O/C ratio of PPEO-High increased from 0.40 to 0.47. However, there was a slight decrease in the O-ratio of PPEO-Low from 0.35 to 0.31, which was attributed to dissolution of high molecular weight oligomeric chains. In the case of PPEN-High and PPEN-Low, the O/C ratio increased from 0.02 to 0.16, and 0.01 to 0.18, respectively. The N/C ratio for PPEN-High and PPEN-Low decreased from 0.18 to 0.09 in both the samples. In the case of PPES-High and PPES-Low, the O/S ratio increased from 0.25 to 0.75, and 0.10 to 0.12, respectively. The S/C ratio decreased from 0.14 to 0.12 and 0.24 to 0.22, for PPES-High and PPES-Low respectively. This does show that there is some reduction observed in the chemical groups, but they are not destroyed by the sterilization cycle and PPES films are the most stable PPFs towards sterilization. After sterilization by a wet heat cycle, the hydrogels with PPFs were seeded with R-LECs on the surface. Five out of eight PPFs favored the attachment and proliferation of cells (compared to the response on untreated hydrogel surface) whereas the other three PPFs displayed the completely opposite result. To understand these observations, various characterization experiments were performed on the eight PPFs.

The first and the most obvious characterization test was done to measure the wettability of the PPFs. Some authors have previously determined that wettability of a given surface is key to control cell attachment and proliferation on the same surface, with cells preferring hydrophilic surfaces over hydrophobic ones [42, 43]. In our study, it could be one reason for the non-attachment observed on PPE-High and PPE-Low surfaces, but it does not explain why untreated hydrogel with a similar WCA supports the attachment and proliferation. Untreated hydrogel, PPE-High and PPE-Low had WCA of 83 ± 5, 87 ± 2 and 80 ± 3 degrees respectively (Fig. 5), but the relative cell attachment on PPE-High and PPE-Low with respect to untreated hydrogel were about 44.98% and 18.55% respectively (Fig. 3). In the O-rich PPFs, the difference in WCA (Fig. 5) and cell attachment levels (Fig. 3) was noticeable. PPEO-High had WCA of 56 ± 3 and relative cell attachment of 160.7%, whereas PPEO-Low had WCA of 75 ± 3 and relative cell attachment of 146.8%. In the case of nitrogen-rich surfaces, the difference between the WCA was small but the difference in cell attachment levels was staggering. PPEN-High was the hydrophobic surface, with WCA of 73 ± 4 compared to 64 ± 4 of PPEN-Low. The relative cell attachment on PPEN-High was 21.64% whereas the 163.1% of PPEN-Low. Similarly, on PPES-High and PPES-Low samples, the WCA were 63 ± 2 and 74 ± 4, respectively whereas the relative cell attachments were 173.0% and 615.3%, respectively. The higher attachment of R-LECs on PPES surfaces could be attributed to the increased adsorption of proteins/growth factors from the media during cell culture [44, 45]. Both the PPES surfaces showed highest immobilization to laminin (Fig. 8) and preferential attachment to BSA (Fig. 7a). With this data, it is difficult to comment if wettability is the only parameter affecting cell attachment and proliferation. Notably, experiments by Bozukova et al. on hydrogel surfaces have shown that in some cases, cell attachment could be enhanced by increasing the hydrophobicity [46]. While this study reports observations on plasma-polymerized C_2H_4 films, we have also carried out some experiments on plasma-polymerized C_4H_6 films and the relation between cell attachment and factors such as wettability, chemical composition and mechanical properties seems multifaceted (*Data included under Appendix II of Supplementary section*).

In an earlier study, we investigated the effect of protein adsorption quantity on monocyte adhesion onto PPFs deposited on BOPP substrates [35]. Older studies have also shown the

effect of pre-adsorbed proteins on cellular adhesion to polymeric substrates [47]. Proteins form the initial film on biomaterial surfaces, whether from media in in-vitro cultures or from body fluids in-vivo and the interaction of cells with these proteins has been suggested to dictate the cell attachment and proliferation process [48]. In this study, BSA was chosen as a key component of the human tear fluid, the primary body fluid that would interact with contact lenses [49, 50]. One key observation held true across the eight PPFs. The PPFs labelled with suffix "Low" were treated under a higher working pressure (80 Pa), lower RF power (10 W) compared to those with suffix "High" (Pressure – 10 Pa, Power – 30 W). In any given type of PPF (hydrocarbon rich, O-rich, or N-rich), the "High" variant displayed Higher adsorption of proteins compared to the "Low" variant of the PPF. Protein adsorption onto a given PPF depends on factors such as electrostatic interactions between the protein and the surface, size of the protein and the pore size of the surface [51]. A common reason for the trend observed across "High" and "Low" PPF variants could very well be the nano topography of the PPFs. While much detail has not been described here, in our earlier study we had shown via electron microscopy images that PPFs formed in Higher pressure, lower RF powers ("Low" variants) are generally smoother in appearance compared to the lower pressure, Higher RF power PPFs ("High" variants) [24]. Indeed, studies have shown that the amount of fouling on a given surface increases proportionally with its roughness [52]. The difference observed in the quantity of BSA adsorbed onto the PPFs can be explained by the formation of charged groups on the PPFs in aqueous solutions [30]. N-rich PPFs form positively charged ammonium groups, attracting the negatively charged BSA better than the O-rich PPFs (Fig. 7a). Pure hydrocarbon PPFs have no native polar groups, but they might form positively charged groups upon exposure to atmospheric nitrogen and therefore end up favoring the adsorption of negatively charged BSA [53].

Analysis of the conformation of BSA on various PPFs did reveal slight changes taking place (Fig. 7c). It is to be noted that other studies have determined the native conformational state of BSA in aqueous solution to be composed of 47% alpha-helices, 3% beta-sheets, 24% coils and 26% non-ordered structures [54]. PPEO-High was the surface that showed conformational state of BSA closest to its native state (41% alpha-helices, 4% beta-sheets, 25% coils and 30% non-ordered structures). All other PPFs showed higher deviation from the native conformational state of BSA. Between the two hydrocarbon-rich PPFs, conformational distribution of BSA across two different states was similar (~38% alpha-helices, 4.7% beta-sheets) whereas the other two states (coils and non-ordered structures) showed differences in the order of 3%. PPEO-Low was quite different from PPEO-High (35% alpha-helices, 6% beta-sheets, 33% coils and 26% non-ordered structures). Between PPEN-High and PPEN-Low, differences of the order of 4% were encountered only in two states (coils and non-ordered structures). PPEO-High had Higher relative cell attachment than PPEO-Low, but it is hard to state if any of these conformational changes were responsible for the difference. Similar observation can be made for PPEN-High and PPEN-Low, with no concrete indication of one single conformational state being responsible for the drastic difference in relative cell attachments.

However, mechanical properties of the PPFs do shed some light on the relative cell attachments of the N-rich films. PPEN-Low films were stiffer compared to PPEN-High films, possessing higher elastic modulus and indentation hardness. The slight increase in relative cell attachment on PPE-High films compared to PPE-Low could be due to the higher stiffness of PPE-High over PPE-Low films. Earlier studies have shown that films deposited at lower power outputs display higher elastic moduli compared to films deposited at higher power outputs [39]. All PPFs are stiffer than the untreated hydrogel, and this too has been proven in earlier studies. Plasma polymers are composed of random, denser

crosslinked units compared to conventional polymers and this explains the change in mechanical properties [55]. If we consider PPE-Low, the incorporation of both oxygen and nitrogen into the PPE films produced at same RF output power and working pressure led to increases in elastic modulus and hardness. Similar findings were reported for HMDSO–O_2 and C_2H_4–N_2 films [56, 57]. However, PPE-High was stiffer than PPEO-High and PPEN-High. The amount of sp^3 carbon, degree of branching and crosslinking affect the mechanical properties of PPFs and more in-depth study is needed to explain this observation [58].

Mechanical properties of the scaffold surface have been shown to influence the attachment and proliferation of some types of cells [59]. In another example, stiffness was shown to be the prime factor behind the response of cells [60]. However, in another study, PPFs deposited from oxazoline were almost similar in stiffness but showed a glaring difference in the relative viabilities of the cells grown on the different PPFs [61]. Therefore, it does appear that cell interaction with any scaffold surface is dependent on a complex interplay of factors, and it is not possible to determine the compatibility of a surface based on its wettability alone. Particularly, we have shown that in the case of N-rich films, it is possible to achieve both ends of the spectrum in terms of cell attachment by changing the plasma processing parameters even though both the films possess similar surface chemistry (Table 2). Earlier studies had concluded a minimum threshold of N% necessary to support proliferation of certain types of cells, but as we expand the study to include more cells, mechanical and other properties of PPFs come into play [62]. Future studies could therefore be directed towards understanding expression of epithelial cell markers such as EpCam to understand changes occurring in R-LECs upon exposure to different PPFs.

Immobilization of laminin was found to be highest on PPES surfaces. Both the PPES surfaces showed high amount of laminin immobilization, and this resulted in higher cell attachment compared to surfaces with no immobilized laminin. Surfaces with sulfur-rich groups have been known to display high affinity for proteins, and this explains the higher immobilization of laminin on PPES surfaces compared to other PPFs [63]. The high affinity could possibly be due to the formation of disulfide bonds between proteins and the sulfur-rich surfaces [64]. There was a difference in the cell attachment levels between the two types of surfaces, and this could be attributed to changes produced in the conformation of immobilized laminin [65]. Sulfur containing groups are widespread in biological systems, and mediate adhesion between protein ligands [66]. This shows the possibility of usage of PPES surfaces in applications involving biomolecule immobilization on hydrogels and biomaterials surfaces.

Conclusion

Plasma processing parameters for creating water stable and steam-sterilisation resistant PPFs on hydrogels were studied. Such films were able to obtain a range of wettability values, protein adsorption characteristics and mechanical property values. These properties provided control over a range of cell proliferation situations. O-rich films have shown the ability to enhance cell attachment by a factor of 1.5–1.6, irrespective of the plasma processing parameters. Interestingly, N-rich films could be used as cell attachment enhancing films (1.6 times untreated hydrogel) as well as anti-fouling coatings (0.25 times untreated hydrogel). S-rich conditions can also be used to enhance cell attachment by factor ranging from 2× to 6× that of an untreated hydrogel surface. The films were also used to covalently immobilise laminin, and further enhance cell proliferation and allow control over the type

of biomolecule being adsorbed on the contact lens surface. Such surface modified hydrogels could be used as cell therapy transfer options to the eye or other parts of the body.

Supplementary Information The online version contains supplementary material available at https://doi.org/10.1007/s11090-023-10319-w.

Acknowledgements The authors would like to thank Lisa Danielczak for training and support, and Prof. Richard Leask for granting generous access to his laboratory facilities for cell culture studies.

Author Contributions The manuscript was written through contributions of all authors. All authors have given approval to the final version of the manuscript.

References

1. Zhang LF, Yang DJ, Chen HC, Sun R, Xu L, Xiong ZC, Govender T, Xiong CD (2008) An ionically crosslinked hydrogel containing vancomycin coating on a porous scaffold for drug delivery and cell culture. Int J Pharm 353:74–87
2. Chen Y-M, Yang J-J, Osada Y, Gong JP (2010) Synthetic hydrogels as scaffolds for manipulating endothelium cell behaviors. Chin J Polym Sci 29:23–41
3. Hassan E, Deshpande P, Claeyssens F, Rimmer S, Macneil S (2014) Amine functional hydrogels as selective substrates for corneal epithelialization. Acta Biomater 10:3029–3037
4. Schulz A, Gepp MM, Stracke F, Von Briesen H, Neubauer JC, Zimmermann H (2019) Tyramine-conjugated alginate hydrogels as a platform for bioactive scaffolds. J Biomed Mater Res A 107:114–121
5. Drury JL, Mooney DJ (2003) Hydrogels for tissue engineering: scaffold design variables and applications. Biomaterials 24:4337–4351
6. Janse Van Rensburg A, Davies NH, Oosthuysen A, Chokoza C, Zilla P, Bezuidenhout D (2017) Improved vascularization of porous scaffolds through growth factor delivery from heparinized polyethylene glycol hydrogels. Acta Biomater 49:89–100
7. Geckil H, Xu F, Zhang X, Moon S, Demirci U (2010) Engineering hydrogels as extracellular matrix mimics. Nanomedicine (Lond) 5:469–484
8. Tibbitt MW, Anseth KS (2009) Hydrogels as extracellular matrix mimics for 3D cell culture. Biotechnol Bioeng 103:655–663
9. Yuan X, Wei Y, Villasante A, Ng JJD, Arkonac DE, Chao PG, Vunjak-Novakovic G (2017) Stem cell delivery in tissue-specific hydrogel enabled meniscal repair in an orthotopic rat model. Biomaterials 132:59–71
10. Blache U, Ehrbar M (2018) Inspired by nature: hydrogels as versatile tools for vascular engineering. Adv Wound Care (New Rochelle) 7:232–246
11. Stratakis E (2018) Novel biomaterials for tissue engineering 2018. Int J Mol Sci 19:3960
12. Assuncao-Silva RC, Gomes ED, Sousa N, Silva NA, Salgado AJ (2015) Hydrogels and cell based therapies in spinal cord injury regeneration. Stem Cells Int 2015:948040
13. Haile Y, Berski S, Drager G, Nobre A, Stummeyer K, Gerardy-Schahn R, Grothe C (2008) The effect of modified polysialic acid based hydrogels on the adhesion and viability of primary neurons and glial cells. Biomaterials 29:1880–1891
14. Hejcl A, Ruzicka J, Kapcalova M, Turnovcova K, Krumbholcova E, Pradny M, Michalek J, Cihlar J, Jendelova P, Sykova E (2013) Adjusting the chemical and physical properties of hydrogels leads to improved stem cell survival and tissue ingrowth in spinal cord injury reconstruction: a comparative study of four methacrylate hydrogels. Stem Cells Dev 22:2794–2805
15. Bobba, S, Di Girolamo N, Watson S (2016) Contact lens delivery of stem cells for restoring the ocular surface. In: Biomaterials and regenerative medicine in ophthalmology. pp 219–239
16. Deshpande P, Notara M, Bullett N, Daniels JT, Haddow DB, Macneil S (2009) Development of a surface-modified contact lens for the transfer of cultured limbal epithelial cells to the cornea for ocular surface diseases. Tissue Eng Part A 15:2889–2902
17. Brown KD, Low S, Mariappan I, Abberton KM, Short R, Zhang H, Maddileti S, Sangwan V, Steele D, Daniell M (2014) Plasma polymer-coated contact lenses for the culture and transfer of corneal epithelial cells in the treatment of limbal stem cell deficiency. Tissue Eng Part A 20:646–655

18. Kushnerev E, Shawcross SG, Sothirachagan S, Carley F, Brahma A, Yates JM, Hillarby MC (2016) Regeneration of corneal epithelium with dental pulp stem cells using a contact lens delivery system. Invest Ophthalmol Vis Sci 57:5192–5199
19. Masoudi S, Stapleton FJ, Willcox MDP (2016) Contact lens-induced discomfort and protein changes in tears. Optom Vis Sci 93:955–962
20. Chen JW, Lim K, Bandini SB, Harris GM, Spechler JA, Arnold CB, Fardel R, Schwarzbauer JE, Schwartz J (2019) Controlling the surface chemistry of a hydrogel for spatially defined cell adhesion. ACS Appl Mater Interfaces 11:15411–15416
21. Ino JM (2013) Plasma functionalization of poly(vinyl alcohol) hydrogel for cell adhesion enhancement. Biomatter 3:e25414
22. Bayramoglu G, Bitirim V, Tunali Y, Arica MY, Akcali KC (2013) Poly (hydroxyethyl methacrylate-glycidyl methacrylate) films modified with different functional groups: In vitro interactions with platelets and rat stem cells. Mater Sci Eng C Mater Biol Appl 33:801–810
23. Kim HH, Park JB, Kang MJ, Park YH (2014) Surface-modified silk hydrogel containing hydroxyapatite nanoparticle with hyaluronic acid-dopamine conjugate. Int J Biol Macromol 70:516–522
24. Rout B, Girard-Lauriault PL (2021) Permeation-resistant and flexible plasma-polymerised films on 2-hydroxyethyl methacrylate hydrogels. Plasma Process Polym 18:2000191
25. Wang YM, Qian XF, Zhang XF, Xia W, Zhong L, Sun ZT, Xia J (2013) Plasma surface modification of rigid contact lenses decreases bacterial adhesion. Eye Contact Lens-Sci Clin Pra 39:376–380
26. Zhang LH, Wu D, Chen YS, Wang XL, Zhao GW, Wan HY, Huang CZ (2009) Surface modification of polymethyl methacrylate intraocular lenses by plasma for improvement of antithrombogenicity and transmittance. Appl Surf Sci 255:6840–6845
27. Wang P, Tan KL, Kang ET, Neoh KG (2002) Plasma-induced immobilization of poly(ethylene glycol) onto poly(vinylidene fluoride) microporous membrane. J Membr Sci 195:103–114
28. Ademovic Z, Holst B, Kahn RA, Jorring I, Brevig T, Wei J, Hou X, Winter-Jensen B, Kingshott P (2006) The method of surface PEGylation influences leukocyte adhesion and activation. J Mater Sci-Mater Med 17:203–211
29. Buddhadasa M, Girard-Lauriault P-L (2015) Plasma co-polymerisation of ethylene, 1,3-butadiene and ammonia mixtures: Amine content and water stability. Thin Solid Films 591:76–85
30. Babaei S, Girard-Lauriault P-L (2016) Tuning the surface properties of oxygen-rich and nitrogen-rich plasma polymers: functional groups and surface charge. Plasma Chem Plasma Process 36:651–666
31. Girard-Lauriault P-L, Mwale F, Iordanova M, Demers C, Desjardins P, Wertheimer MR (2005) Atmospheric pressure deposition of micropatterned nitrogen-rich plasma-polymer films for tissue engineering. Plasma Process Polym 2:263–270
32. Hegedus O, Juriga D, Sipos E, Voniatis C, Juhasz A, Idrissi A, Zrinyi M, Varga G, Jedlovszky-Hajdu A, Nagy KS (2019) Free thiol groups on poly(aspartamide) based hydrogels facilitate tooth-derived progenitor cell proliferation and differentiation. PLoS ONE 14:e0226363
33. Galli C, Parisi L, Elviri L, Bianchera A, Smerieri A, Lagonegro P, Lumetti S, Manfredi E, Bettini R, Macaluso GM (2016) Chitosan scaffold modified with D-(+) raffinose and enriched with thiol-modified gelatin for improved osteoblast adhesion. Biomed Mater 11:015004
34. Wargenau A, Fekete N, Beland AV, Sabbatier G, Bowden OM, Boulanger MD, Hoesli CA (2019) Protein film formation on cell culture surfaces investigated by quartz crystal microbalance with dissipation monitoring and atomic force microscopy. Colloids Surf B Biointerfaces 183:110447
35. Babaei S, Fekete N, Hoesli CA, Girard-Lauriault PL (2018) Adhesion of human monocytes to oxygen- and nitrogen- containing plasma polymers: effect of surface chemistry and protein adsorption. Colloids Surf B Biointerfaces 162:362–369
36. Ratner BD, Horbett T, Hoffman AS, Hauschka SD (1975) Cell adhesion to polymeric materials: implications with respect to biocompatibility. J Biomed Mater Res 9:407–422
37. Carette X, Mincheva R, Herbin M, Cabecas Segura P, Wattiez R, Noirfalise X, Thai C, Leclere P, Godfroid T, Boudifa M, Kerdjoudj H, Jolois O, Raquez JM (2021) Microwave atmospheric plasma: a versatile and fast way to confer antimicrobial activity toward direct chitosan immobilization onto poly(lactic acid) substrate. ACS Appl Bio Mater 4:7445–7455
38. Olivero DK, Furcht LT (1993) Type IV collagen, laminin, and fibronectin promote the adhesion and migration of rabbit lens epithelial cells in vitro. Invest Ophthalmol Vis Sci 34:2825–2834
39. Beake BD, Zheng S, Alexander MR (2002) Nanoindentation testing of plasma-polymerised hexane films. J Mater Sci 37:3821–3826
40. Castillo EJ, Koenig JL, Andersen JM, Lo J (1984) Characterization of protein adsorption on soft contact lenses: I. Conformational changes of adsorbed human serum albumin. Biomaterials 5:319–325
41. Surewicz WK, Mantsch HH (1988) New insight into protein secondary structure from resolution-enhanced infrared spectra. Biochim Biophys Acta BBA Protein Struct Mol Enzymol 952:115–130

42. Lin C-H, Jao W-C, Yeh Y-H, Lin W-C, Yang M-C (2009) Hemocompatibility and cytocompatibility of styrenesulfonate-grafted PDMS-polyurethane-HEMA hydrogel. Colloids Surf B 70:132–141
43. D'sa RA, Raj J, Mcmahon MA, Mcdowell DA, Burke GA, Meenan BJ (2012) Atmospheric pressure plasma induced grafting of poly(ethylene glycol) onto silicone elastomers for controlling biological response. J Colloid Interface Sci 375:193–202
44. Webb K, Hlady V, Tresco PA (2000) Relationships among cell attachment, spreading, cytoskeletal organization, and migration rate for anchorage-dependent cells on model surfaces. J Biomed Mater Res 49:362–368
45. Webb K, Hlady V, Tresco PA (1998) Relative importance of surface wettability and charged functional groups on NIH 3T3 fibroblast attachment, spreading, and cytoskeletal organization. J Biomed Mater Res 41:422–430
46. Bozukova D, Pagnoulle C, De Pauw-Gillet M-C, Klee D, Dupont-Gillain C, Duwez A-S, Gilbert Y, Jerome R, Jerome C (2010) Plasma surface fluorination of hydrogel materialscoating stability and in vitro biocompatibility testing. Soft Mater 8:164–182
47. Tamada Y, Ikada Y (1993) Effect of preadsorbed proteins on cell adhesion to polymer surfaces. J Colloid Interface Sci 155:334–339
48. Wilson CJ, Clegg RE, Leavesley DI, Pearcy MJ (2005) Mediation of biomaterial-cell interactions by adsorbed proteins: A review. Tissue Eng 11:1–18
49. De Souza GA, Godoy LM, Mann M (2006) Identification of 491 proteins in the tear fluid proteome reveals a large number of proteases and protease inhibitors. Genome Biol 7:R72
50. Luensmann D, Heynen M, Liu L, Sheardown H, Jones L (2010) The efficiency of contact lens care regimens on protein removal from hydrogel and silicone hydrogel lenses. Mol Vis 16:79–92
51. Omali NB, Subbaraman LN, Coles-Brennan C, Fadli Z, Jones LW (2015) Biological and clinical implications of lysozyme deposition on soft contact lenses. Optom Vis Sci Off Publ Am Acad Optom 92:750–757
52. Rana D, Matsuura T (2010) Surface modifications for antifouling membranes. Chem Rev 110:2448–2471
53. Truica-Marasescu F, Wertheimer MR (2008) Nitrogen-rich plasma-polymer films for biomedical applications. Plasma Process Polym 5:44–57
54. Surewicz WK, Mantsch HH, Chapman D (1993) Determination of protein secondary structure by Fourier transform infrared spectroscopy: A critical assessment. Biochemistry 32:389–394
55. Trivedi R, Cech V (2010) Mechanical properties of plasma polymer film evaluated by conventional and alternative nanoindentation techniques. Surf Coat Technol 205:S286–S289
56. BenítEz F, MartíNez E, Esteve J (2000) Improvement of hardness in plasma polymerized hexamethyldisiloxane coatings by silica-like surface modification. Thin Solid Films 377–378:109–114
57. Almeida LS, Souza ARM, Costa LH, Rangel EC, Manfrinato MD, Rossino LS (2020) Effect of nitrogen in the properties of diamond-like carbon (DLC) coating on Ti6Al4V substrate. Mater Res Express 7:065601
58. Thiry D, De Vreese A, Renaux F, Colaux JL, Lucas S, Guinet Y, Paccou L, Bousser E, Snyders R (2016) Toward a better understanding of the influence of the hydrocarbon precursor on the mechanical properties of a-C: H coatings synthesized by a hybrid PECVD/PVD method. Plasma Process Polym 13:316–323
59. Fereol S, Fodil R, Labat B, Galiacy S, Laurent VM, Louis B, Isabey D, Planus E (2006) Sensitivity of alveolar macrophages to substrate mechanical and adhesive properties. Cell Motil Cytoskeleton 63:321–340
60. Hopp I, Michelmore A, Smith LE, Robinson DE, Bachhuka A, Mierczynska A, Vasilev K (2013) The influence of substrate stiffness gradients on primary human dermal fibroblasts. Biomaterials 34:5070–5077
61. Stahel P, Mazankova V, Tomeckova K, Matouskova P, Brablec A, Prokes L, Jurmanova J, Bursikova V, Pribyl R, Lehocky M, Humpolicek P, Ozaltin K, Trunec D (2019) Atmospheric pressure plasma polymerized oxazoline-based thin films-antibacterial properties and cytocompatibility performance. Polymers (Basel) 11:2069
62. Girard-Lauriault P-L, Truica-Marasescu F, Petit A, Wang HT, Desjardins P, Antoniou J, Mwale F, Wertheimer MR (2009) Adhesion of human U937 monocytes to nitrogen-rich organic thin films: Novel insights into the mechanism of cellular adhesion. Macromol Biosci 9:911–921
63. Alibeik S, Rizkalla AS, Mequanint K (2007) The effect of thiolation on the mechanical and protein adsorption properties of polyurethanes. Eur Polym J 43:1415–1427
64. Summonte S, Racaniello GF, Lopedota A, Denora N, Bernkop-Schnurch A (2021) Thiolated polymeric hydrogels for biomedical application: Cross-linking mechanisms. J Control Release 330:470–482

65. Fischer NG, He J, Aparicio C (2020) Surface immobilization chemistry of a laminin-derived peptide affects keratinocyte activity. Coatings (Basel) 10:560
66. Siow KS, Britcher L, Kumar S, Griesser HJ (2017) Plasma polymers containing sulfur and their copolymers with 1,7-octadiene: chemical and structural analysis. Plasma Process Polym 14:1600044